Development and Assessment of a Higher Spatial Resolution (4.4 km) MISR Aerosol Optical Depth Product Using AERONET-DRAGON Data

Michael J. Garay[1], Olga V. Kalashnikova[1], and Michael A. Bull[1]

[1]{Jet Propulsion Laboratory, California Institute of Technology, Pasadena, California}

Correspondence to: M. J. Garay (Michael.J.Garay@jpl.nasa.gov)

Abstract

Since early 2000, the Multi-angle Imaging SpectroRadiometer (MISR) instrument on NASA's Terra satellite has been acquiring data that has been used to produce aerosol optical depth (AOD) and particle property retrievals at 17.6 km spatial resolution. Capitalizing on the capabilities provided by multiangle viewing, the current operational (Version 22) MISR algorithm performs well with about 75% of MISR AOD retrievals globally falling within 0.05 or 20% × AOD of paired validation data from the ground-based Aerosol Robotic Network (AERONET). This paper describes the development and assessment of a prototype version of a higher spatial resolution, 4.4 km MISR aerosol optical depth product compared against multiple AERONET Distributed Regional Aerosol Gridded Observations Network (DRAGON) deployments around the globe. In comparisons with AERONET-DRAGON AODs the 4.4 km resolution retrievals show improved correlation (r = 0.9595), smaller root mean squared error (0.0768), reduced bias (-0.0208), and a larger fraction within the expected error envelope (80.92%) relative to the Version 22 MISR retrievals.

1 Introduction

Atmospheric aerosols, suspended particles of solid and liquid, play key roles in the weather and climate of the Earth. Aerosol optical depth (AOD) is a fundamental parameter that expresses the amount of aerosol in the atmospheric column and its effect on the transmission of sunlight. Global observations of aerosol amount depend fundamentally on retrievals of

AOD from instruments on satellite platforms, such as Multi-angle Imaging SpectroRadiometer (MISR) and the MODerate resolution Imaging Spectroradiometer (MODIS) that fly on the NASA Earth Observing System (EOS) Terra satellite. Satellite aerosol observations are used to model the global radiation budget and investigate the effects of aerosols on clouds (e.g., Boucher et al., 2013). Applications of satellite-derived AOD information include air quality and health studies that use satellite-retrieved AOD to estimate ground-level concentrations of particulate matter, especially particles with aerodynamic diameter less than 2.5 μm ($PM_{2.5}$), which are known to have significant health effects due to their ability to penetrate the human respiratory system (e.g., Martin, 2008; van Donkelaar et al., 2015; 2016).

Critical to the success of satellite aerosol missions like MISR and MODIS are assessments of the performance of their retrieval algorithms. Algorithm performance is typically evaluated by the ability of the retrievals to capture the observed spatiotemporal variability of aerosols as determined by ground-based observations, which are taken to represent the "truth." Within the satellite aerosol community, the Aerosol Robotic Network (AERONET) is often used as a standard, global reference. AERONET is a federated instrument network of ground-based sunphotometers that derive AOD at a number of visible and near-infrared wavelengths from direct sun observations (Holben et al., 1998).

The MISR instrument has been acquiring data from on board the NASA Terra Earth Observing System (EOS) platform since early 2000. The current Level 2 (swath-based) aerosol retrieval algorithm, designated F12_0022, or Version 22 (V22), began production at the NASA Langley Research Center Atmospheric Science Data Center (ASDC) on 1 December 2007, and has been applied to the entire MISR mission, including operational (forward) processing. Details of the V22 MISR aerosol retrieval over water and land can be found in Kalashnikova et al. (2013) and Martonchik et al. (2009), respectively. AOD and associated aerosol particle properties are reported in the MISR aerosol product on a 17.6 km spatial resolution grid, which represents 16 × 16 (256) samples of the 1.1 km resolution MISR observations in four spectral bands in the visible and near infrared made from nine separate viewing angles (Diner et al., 1998). The MISR aerosol product was evaluated against global AERONET sites by Kahn et al. (2010), who reported that, overall, about 70% to 75% of MISR AOD retrievals are within the greater of 0.05 or 0.2 × AOD of the paired AERONET data. By way of comparison, the operational MODIS Collection 6 (C6) Dark Target (DT)

algorithm, which began production in 2014, has a reported expected error (EE) envelope, containing about 67% of the retrievals relative to AERONET, of –(0.02 + 0.1 × AOD) to +(0.04 + 0.1 × AOD) (Levy et al., 2013). Sayer et al. (2015) found that about 85% of vegetated sites and 70% of arid sites fell within the EE envelope of ±(0.05 + 0.2 × AOD) for the MODIS C6 Deep Blue (DB) algorithm for MODIS-Terra after the application of calibration corrections for the sensor.

Kahn et al. (2010) also identified a number of issues in the performance of the V22 MISR aerosol retrieval algorithm, including: lack of extremely low AODs in the MISR data compared to AERONET that causes an apparent "gap" in the comparison plots; the appearance of quantization noise; lack of particle types in the aerosol look up table to adequately represent all naturally occurring aerosol types; and a frequent underestimate of AOD relative to AERONET over land when the AOD is greater than about 0.4. The authors speculated that this underestimate was due to insufficiently absorbing particles being selected in cases where absorbing aerosols were present, or AOD variability at the 17.6 km spatial scale of the retrieval being incorrectly treated as surface variability reducing the contribution of aerosols to the top-of-atmosphere reflectances, resulting in a systematic underestimation of the AOD in these situations. Subsequently, Kalashnikova et al. (2013), Witek et al. (2013), and Shi et al. (2014) identified issues with the cloud screening applied in the V22 algorithm, especially with regard to thin cirrus, and suggested possible solutions; and Limbacher and Kahn (2015) diagnosed the effects of stray light in the MISR cameras, noted earlier by Bruegge et al. (2002), that could have significant impact on retrieved AODs in scenes with high contrast. These efforts by members of the MISR science team and others have been directed at improving the quality of the MISR aerosol product with the view of delivering a new version of the operational MISR aerosol retrieval algorithm in the near future. At the same time, a number of studies have highlighted the need for aerosol products at higher spatial resolutions than currently available operationally from MISR and MODIS, gridded at 17.6 km and 10.0 km, respectively. In response to this, the MODIS team released a global 3 km resolution DT aerosol product as part of its Collection 6 delivery (Remer et al., 2013). In this work, we describe the effort to develop a higher resolution, 4.4 km Level 2 MISR aerosol product based on initial tests that showed significant AOD retrieval improvement relative to AERONET sites deployed in relatively large numbers locally in Distributed Regional Aerosol Gridded Observations Network (DRAGON) campaigns in regions around the globe (e.g., Eck

et al., 2014; Seo et al., 2015; Sano et al., 2016). In the DRAGON networks, instruments are located much closer to one another, with a typical grid spacing around 10 km (e.g., Munchak et al., 2013). As we will discuss in this paper, we found that a MISR 4.4 aerosol retrieval using the same algorithm as the operational (V22) 17.6 km product is better able to resolve spatial gradients in AOD as shown in a number of comparisons from different DRAGON deployments that encompass a wide range of aerosol loadings.

2 Data and methods

2.1 20 January 2013 MISR overpass of DRAGON San Joaquin Valley, California

The initial motivation for this work was a MISR overpass of the DRAGON sites deployed in the San Joaquin Valley of California in support of the NASA Deriving Information on Surface conditions from Column and Vertically Resolved Observations Relevant to Air Quality (DISCOVER-AQ) field campaign in January and February 2013 (see Beyersdorf et al., 2016). Figure 1a shows the red band (672 nm) image from MISR orbit 69644 when the Terra satellite passed over the San Joaquin Valley around 18:50 UTC on 20 January 2013. The image is oriented with north to the top. The bright features in the upper central portion of the image are snow in the Sierra Nevada, with the San Joaquin Valley of Central California to the southwest. Figure 1b shows the green band (558 nm) AOD reported in the MISR V22 operational aerosol product at 17.6 km resolution. The circles correspond to the AODs reported by the AERONET-DRAGON sites closest in time to the Terra overpass using the same color scale as the MISR AODs. The horizontal lines denote the MISR "blocks" that correspond to 141 km in the along-track direction of the satellite motion (Bothwell et al., 2002). It is clear in Fig. 1b that the aerosols are concentrated in the San Joaquin Valley, although on this date the AOD is relatively low, with a maximum around 0.30.

As mentioned above, the V22 MISR aerosol retrieval algorithm takes as input the 256 – 1.1 km MISR Level 1B2 pixels within the 17.6 km retrieval region (16 pixels × 16 pixels). In standard "global" acquisition mode, blue, green, and near infrared bands in the off-nadir cameras are averaged onboard from the full 275 m pixel resolution to 1.1 km to save data rate, while the red bands in all nine cameras and the blue, green, and near infrared bands for the nadir camera are preserved at their full resolution (Diner et al., 1998). The 1.1 km pixel data

for the red band and the nadir camera is calculated by the aerosol algorithm by simple averaging. The MISR instrument has another "local" acquisition mode that preserves the full (275 m) resolution of the data for all nine cameras and four spectral bands for a target with an along-track length of about 300 km (Diner et al., 1998). It was recognized that with some modifications to deal with the new inputs the V22 aerosol retrieval algorithm could be applied to "local mode" data, resulting in a product with 4.4 km spatial resolution due to the change of the input resolution from 1.1 km to 275 m (since 275 m × 16 = 4.4 km). Figure 1c shows the results of the application of the V22 algorithm to a local mode acquisition made over Pixley, CA (PIXLEYCA), which accounts for the smaller geographic coverage of the retrieval. The same color scale is applied to the AOD retrievals in this case as in Fig. 1b, and, again, the AERONET-DRAGON sites are indicated by circles colored by the AOD reported for the time nearest the Terra overpass. Not only is much greater detail revealed regarding the spatial distribution of aerosols in the San Joaquin Valley, with higher aerosol loading extending from the Fresno in the central part of the valley to Bakersfield in the southeast, but visually the agreement between the MISR AODs and the AERONET-DRAGON AODs is much improved.

The visual impression of better agreement is borne out in the analysis shown in Fig. 2. Figure 2a compares the 17.6 km V22 AODs from MISR at 558 nm with the AERONET AODs linearly interpolated from the two nearest wavelengths on either side in log-log space to 558 nm (e.g., Sayer et al., 2013). The matches are made nearest in time to the Terra overpass (typically within 15 minutes) and the AERONET observations are required to fall within a specific 17.6 km retrieval region. These criteria are somewhat different than the matching criteria used in Kahn et al. (2010), who considered the average AOD of AERONET observations within a 2 h window centered at the time of the satellite overpass, with at least one valid observations within the hour before and one in the hour after, and also considered MISR retrievals in both the "central" 17.6 km region and the eight surrounding regions. The interpolation of the AERONET AODs to the MISR wavelength was also done slightly differently using a second order polynomial fit, but this resulted in a negligible change in the results in this particular case. As in Kahn et al. (2010) the analysis here uses the "best-estimate" MISR AODs, which correspond to the mean of the AODs for all the mixtures in the MISR look up table that pass the acceptance criteria. For the 17.6 km MISR retrieval there are 11 temporal and spatial matches with the AERONET data. The correlation coefficient, r, is 0.6563; the root mean squared error (RMSE) is 0.0499; the bias is -0.0233; and the percent

of data within the EE envelope of MISR (the greater of 0.05 or 0.20 × AOD) is 72.73%. These results show the 17.6 km V22 retrieval performs relative to the AERONET-DRAGON observations in a way that is generally consistent with the global performance of the algorithm as assessed by Kahn et al. (2010).

Figure 2b shows the comparison of the 4.4 km MISR AODs against the AERONET-DRAGON results using the V22 algorithm with 275 m local mode input. Now the correlation coefficient is 0.9144, the RMSE is 0.0184, the bias is -0.0060, and 100% of the data fall within the EE envelope. These are all significant improvements in the agreement between the MISR AOD retrieval and AERONET-DRAGON. The sampling was reduced by two, but inspection of the results shows that the data points that were eliminated due to the requirement that the AERONET site fall within the 4.4 km retrieval region were both already in good agreement with the 17.6 km MISR aerosol retrieval, which means that the improvement is not simply due to the exclusion of outliers in the comparison. Over years of refinements applied to the 17.6 km algorithm to improve AOD retrieval performance relative to AERONET, the results in Fig. 2 are among the most significant improvements that were ever obtained. Note that these results are also in contrast to the results of Remer et al. (2013) regarding the MODIS 3 km DT retrievals, who reported that agreement of the 3 km retrieval relative to AERONET was slightly worse over land compared to the 10 km retrieval, while the performance was similar over ocean. The EE envelopes were found to be ±0.05 ±0.20 × AOD and ±0.03 ±0.05 × AOD for land and ocean, respectively.

A further point is that the unique, high density nature of the AERONET-DRAGON deployment is important for adequately assessing the ability of a high resolution aerosol retrieval algorithm to capture the true spatial variability of aerosols within a region. As shown in Fig. 1, the higher resolution MISR AOD retrieval is better able to represent the spatial gradients in the aerosol load even though the aerosol load is relatively low on this date and aerosols are spread throughout the San Joaquin Valley. In this case, both the 17.6 km and 4.4 km retrievals report nearly identical values for the Fresno_2 site AERONET site, which is the “permanent” site in the San Joaquin Valley and not part of the DRAGON deployment. So comparisons with this single site alone would not reveal any important difference in the two retrievals. Of course, a single case cannot support the conclusion that the 4.4 km MISR retrieval is superior to the 17.6 km retrieval in an overall sense, so further comparisons were made with AERONET-DRAGON deployments around the globe in a variety of aerosol

loading situations. Even so, the results from the 20 January 2013 case were sufficiently encouraging to focus the MISR science team on the development of a 4.4 km spatial resolution retrieval that would not rely on local mode data to achieve the resolution improvement, but would work with the 1.1 km global mode data as input.

2.2 AERONET-DRAGON deployments

According to the AERONET website (http://aeronet.gsfc.nasa.gov/new_web/dragon.html), there have been nine AERONET-DRAGON deployments between 2011 and 2016. However, the 20 January 2013 MISR case was instructive in terms of specific characteristics of a deployment necessary to facilitate a comparison of the V22 17.6 km resolution aerosol retrieval with a higher resolution 4.4 km retrieval. The primary consideration involves the number and density of sites in the deployment. Table 1 shows an evaluation of eight of the nine DRAGON deployments in terms of the spatial statistics. The on-going deployment of DRAGON as part of the KORUS-AQ field campaign in South Korea, Japan, and China was not considered here.

Starting with the San Joaquin Valley deployment, the Table shows that 28 sites were deployed. This results in 378 pairs (28 choose 2). Calculating the separation between each pair, there are seven pairs separated by less than 17.6 km, 3 pairs separated by less than 8.8 km, and 1 pair separated by less than 4.4 km. The mean distance between pairs is 245.7 km, while the median distance is 204.8 km. The MISR analysis is facilitated by a relatively large number of pairs separated by less than 17.6 km that can be used to test the ability of the 4.4 km algorithm to retrieve AOD spatial gradients, but few pairs separated by less than 4.4 km, which will likely fall inside a single 4.4 km retrieval region. The swath and orbit characteristics of MISR must also be taken into account. MISR has a swath of about 400 km and Terra has a repeat cycle of 16 days. Deployments with widely separated clusters of sites will therefore only provide a limited number of comparisons on a particular MISR overpass. Cloudiness is a further consideration as the DRAGON deployments typically happen within a limited time frame, about a month in the case of the San Joaquin Valley.

Based on these considerations, and visual inspections of candidate scenes, a set of MISR cases was identified during DRAGON deployments for testing the 4.4 km resolution aerosol AOD retrieval performance relative to AERONET in comparison to the 17.6 km resolution AOD retrieval. This set is shown in Table 2. In the table, the “SOM Path” corresponds to the

Space-Oblique Mercator (SOM) projection onto the World Geodetic System 1984 (WGS84) ellipsoid used for the MISR processing (Diner et al., 1998). There are 233 SOM paths within each 16-day repeat cycle of Terra. The cases are broadly classified in terms of the range of AODs, with "low AOD" representing AODs generally less than 0.3, "moderate AOD" corresponding to AODs between about 0.3 and 0.6, and "high AOD" having AODs between about 0.6 and 1.4. Note that while the cases are distributed globally including Washington D.C./Baltimore; the San Joaquin Valley in California; Seoul, South Korea; and Osaka, Japan; a limitation of this study is that the AERONET-DRAGON deployments have been primarily to mid-latitude locations, so there are no cases from tropical, arid desert, or polar regions. Additionally, certain AOD ranges occur preferentially for different DRAGON deployments, with the highest AODs occurring in South Korea.

Figure 3 provides maps of the four relevant AERONET-DRAGON deployments. Figure 3a shows the locations of 45 of the 46 sites deployed in 2011 for the Washington, D.C./Baltimore campaign. The sites are generally located around the greater Baltimore area. For reference, the distance between Washington, D.C. and Baltimore, MD is about 56 km. Also, recall that 1 degree of latitude corresponds to about 111 km. Figure 3b shows the 25 sites deployed in South Korea in 2012. The majority of sites are clustered around Seoul with a relatively large number of sites spaced less than 4.4 km apart, as shown in Table 1. Even so, the overall number of sites makes this a reasonable test case for the 4.4 km MISR aerosol retrieval algorithm. Figure 3c shows the 18 AERONET-DRAGON sites deployed in the San Joaquin Valley of California. Compared to the other cases, the density of sites in this deployment is somewhat smaller, but this provides good sampling of the aerosol distribution throughout the valley. Finally, Fig. 3d shows the locations of the 14 AERONET-DRAGON sites deployed around Osaka, Japan in 2012. The largest density of sites is around Osaka, itself. Again, the spatial clustering of sites is less than ideal, since many are separated by less than 4.4 km.

2.3 MISR aerosol retrievals over land

Details of the MISR aerosol retrieval over land, which is most relevant to comparisons with AERONET-DRAGON, can be found in Martonchik et al. (2009). The fundamental principal of the retrieval is the separation of the multi-angular satellite signal at the top of the atmosphere (TOA) into a component due to the aerosols and a component due to multiple

surface-atmosphere interactions. The primary underlying physical assumptions are the following:

1. Aerosols are horizontally homogeneous in the retrieval region.
2. A predefined set of aerosols stored in a look up table is applied globally to retrievals over both land and water.
3. One or more cost functions (χ^2 parameters) are assessed to determine how well modeled TOA radiances from individual aerosol models and associated green-band AODs match the observed TOA radiances.
4. The angular shape of the surface reflectance is assumed to be spectrally invariant and this is used to filter out models and AODs that do not conform to this assumption as being unlikely candidates for selection (Diner et al., 2005).
5. There is sufficient surface contrast in the retrieval region so that the TOA radiances can be represented by empirical orthogonal functions (EOFs) generated directly from the multiangle imagery.
6. No retrievals are performed over complex terrain (i.e., where the standard deviation of the regional surface elevation exceeds 500 m based on the MISR digital elevation model).

The choice of acceptable 1.1 km subregions within the retrieval region is done through the application of a number of tests including cloud masking. Note that for the comparisons shown in the next section, the aerosol retrieval algorithm was not modified except to provide results at 4.4 km, as opposed to the 17.6 km resolution of the operational retrieval, and the absolute threshold on the χ^2 parameter was relaxed to provide a better match to the coverage of the 17.6 km product. This was required because the value of this threshold was tuned for the 17.6 km product and the coverage of the 4.4 km retrievals was significantly worse in some cases. If anything, adjusting this threshold for the 4.4 km retrievals will allow aerosol models with poorer agreement with the MISR observations to be considered successful.

3 Results

3.1 AOD comparison plots

Figure 4a shows the comparison of the V22 17.6 km MISR green-band AODs against the AERONET-DRAGON AODs interpolated to the MISR wavelength (558 nm) for all the cases listed in Table 2. The range of AODs in this figure is much greater than the AOD range in Fig. 2. Like the comparisons shown in Kahn et al. (2010) the underestimation of the retrieved AODs relative to AERONET for AODs greater than about 0.4 is apparent in this figure. By way of comparison, Fig. 4b shows the results for a prototype 4.4 km MISR aerosol retrieval (internally designated V22b24-34+1) that takes the 1.1 km spatial resolution global mode data as input. Tests showed that the AOD retrievals from this algorithm were not significantly different from the AODs retrieved using the 275 m local mode data as input.

The primary difference apparent in Fig. 4 is the improved performance of the 4.4 km algorithm at high AODs. The fall-off evident in the V22 17.6 km resolution retrievals is greatly mitigated, if not eliminated entirely, but it is difficult to tell if any residual bias exists at large AODs due to the small sample size in this AOD range. Comparing the statistics, the sampling is much greater for the 4.4 km resolution retrieval. This is primarily due to the relaxation of an absolute threshold on the χ^2 parameter to admit similar spatial coverage for the 4.4 km retrieval compared to the 17.6 km retrieval. The need for this change was apparent when looking at maps constructed from the 4.4 km retrievals using the initial threshold. The other parameters all show significant improvements as well. The correlation coefficient goes from 0.8772 to 0.9595; the RMSE decreases from 0.1683 to 0.0768; the bias decreases, in an absolute sense, from –0.0887 to –0.0208, driven primarily by the improvement in the performance of the algorithm at large AODs; and the percent within the MISR EE envelope increases from 59.09% to 80.92%. Although the statistics from this sample are insufficient for a complete analysis, the last result suggests that the performance of the 4.4 km AODs from this algorithm will permit the setting of a somewhat tighter EE envelope, in line with the performance of the MODIS C6 algorithm.

3.2 Example images

Besides providing improved results in AOD when compared with observations from the AERONET-DRAGON sites, the greatest benefit of the 4.4 km resolution MISR aerosol

retrievals is most apparent when comparing maps of the retrieved AOD with the operational V22 17.6 km algorithm. Figure 5 shows the MISR AOD retrievals for Orbit 65731 over Osaka, Japan on 27 April 2012 at about 01:55 UTC. As shown in the MISR red band image in Fig. 5a, the scene is extremely clear. The retrieved AODs on this day range up to about 0.3 in the vicinity of Osaka itself. The main difference between the V22 17.6 km AOD map in Fig. 5b and the 4.4 km retrieval in Fig. 5c is the improvement in coverage due to the relaxation of the absolute χ^2 threshold in the 4.4 km retrieval. The remaining missing retrievals, indicated in white, are due primarily to the shallow water between Honshu, the main landmass in the upper (northern) portion of the image, and the mountainous island of Shikoku. The MISR Dark Water algorithm does not attempt to perform retrievals in locations identified as "shallow water" (water depth less than 50 m) due to possible contributions from reflections from the underwater surface (e.g., Kahn et al., 2009). Retrievals are also not performed over much of Shikoku due to the presence of complex terrain in the mountains, which violates the assumptions of the 1-D radiative transfer used in the MISR aerosol retrieval algorithm. Although these exclusion conditions apply to both the 17.6 km and 4.4 km algorithms, the higher resolution retrieval typically obtains better coverage by being able to get closer to these exclusion zones. Some of the improved coverage of the 17.6 km retrieval, in the lower right portion of the image, in contrast, is only apparent due to the larger area covered by a single 17.6 km pixel, compared to a single 4.4 km pixel.

Figures 6 and 7 show the spatial sampling over South Korea for cases with very high aerosol loads. The white regions in Fig. 6a are clouds to the northeast and southwest of the peninsula on 9 May 2012 at the Terra overpass time around 02:20 UTC. The landmass, however, is mainly clear. The V22 17.6 km retrieval does not have coverage over most of the region, and the agreement between the MISR AODs and the AERONET-DRAGON sites (colored circles) is not particularly good. This result is not particularly surprising given the underestimation at high AODs apparent in Fig. 4a. The 4.4 km aerosol retrieval in Fig. 6b has much better coverage, with the missing locations corresponding well with areas with large amounts of topographic relief. What is particularly striking is the ability of this retrieval to capture the true spatial variability of the aerosol throughout the region, in good agreement with the AERONET-DRAGON observations. In this case, there does not appear to be any high bias due to the presence of urban surfaces, which has been identified as an issue in the MODIS 3 km aerosol product (Munchak et al., 2013). Unfortunately, without ancillary information it is difficult to assess the veracity of the high AODs shown in the vicinity of the clouds in the far

right of the image. However, both the 17.6 km and 4.4 km retrievals indicate elevated AODs in this area.

The case in Fig. 7 has somewhat lower AODs than the previous case. Figure 7a shows the MISR red band image from 25 May 2012 at around 02:20 UTC. There are orographic clouds along the eastern coast of the Korean peninsula and a solid line of clouds in the lower right of the image. Again, the V22 17.6 km resolution product shown in Fig. 7b has missing retrievals over much of the landmass. However, there appears to be a northwest to southeast gradient in the AODs, continuing over the water. Figure 7c shows that evidence for this overall gradient is lacking by filling in many of the missing areas. Instead, locations of high AOD appear sporadically in the scene. The highest AODs are found over Seoul, which has the majority of the AERONET-DRAGON sites, a couple of locations to the southeast, and near the edges of the cloud fields. The two locations to the southeast of Seoul correspond to valleys that are likely trapping pollution on this particular date. Again, it is hard to assess the veracity of the high AODs in the lower portion of the image, but at least the results of the two retrievals are consistent with one another.

4 Discussion and conclusions

The operational V22 MISR aerosol retrieval algorithm went into production in December 2007. Since that time other satellite aerosol retrieval products have undergone significant enhancements, including both the MODIS DT and DB algorithms (Levy et al., 2013; Remer et al., 2013; Sayer et al., 2015). Efforts to improve the MISR aerosol algorithm have focused on the issues noted by Kahn et al. (2010) in their evaluation of the MISR V22 aerosol product against global AERONET observations, as well as topics raised by others (e.g., Kalashnikova et al., 2011; Witek et al., 2013; Shi et al., 2014; and Limbacher and Kahn, 2015). In the meantime, the air quality community has raised the issue of spatial resolution in terms of using satellite data to study the health impacts of atmospheric aerosols on the appropriate "neighborhood scales," on the order of one or a few kilometers.

The biggest surprise in moving the aerosol retrieval to a higher spatial resolution was the improvement in the retrieved AOD relative to AERONET – an improvement that did not require changes to the algorithm itself. This was surprising for two reasons. First, the more or less accepted line of thought was that aerosols are generally spatially homogeneous at scales of 10's to 100's of kilometers, and temporally stationary, in a statistical sense, at time

scales of hours to days (e.g., Anderson et al., 2003). Secondly, the MODIS team did not find significant improvement in the performance of their algorithm when they increased the resolution from 10 km to 3 km (Remer et al., 2013). In fact, this change in resolution highlighted some underlying issues in the assumptions going into the DT retrieval (Munchak et al., 2013). The reasons for the improvement of the MISR AOD retrievals when the spatial resolution is increased from 17.6 km to 4.4 km are complex. The MODIS algorithms rely on assumed relationships in the surface spectral reflectances to account for the lower boundary condition (Levy et al., 2013). Overall, these relationships work well on a global basis, but are apparently adversely affected by the presence of noise, which increases as the resolution increases due to reduction in the spatial averaging. The MISR retrieval approach, on the other hand, attempts to separate the angular contribution from the (assumed variable) surface and the overlying aerosols, which are assumed to be spatially homogeneous (Martonchik et al., 2009). To first order, when the aerosols are not spatially homogeneous then this approach is likely to incorrectly assign this variability to the surface. Kahn et al. (2010) hypothesize that this results in the surface contribution to the top of atmosphere radiances being overestimated, leading the algorithm to retrieve a lower AOD to compensate.

Simply providing results at a higher spatial resolution does not guarantee an improvement in the performance of a satellite retrieval algorithm, however. From a remote sensing standpoint, observations are typically averaged over some spatial scale in an attempt to reduce the impact of random noise in the observations themselves, as in the case of MODIS retrievals. Changes to the resolution can introduce unexpected biases due to changes in the assumptions (e.g., spatial homogeneity, spectral relationships) developed and implemented for coarser resolution retrievals. Importantly, it would have been difficult to assess the performance of a high-resolution algorithm without appropriate high-resolution observations to evaluate against. A single AERONET site basically returns a "point" in space and time relative to retrievals from a satellite instrument. This has led to the adoption of averaging approaches that require large amounts of paired satellite-AERONET data matched within relative broad spatial and temporal windows (e.g., Ichoku et al., 2003; Kahn et al., 2010; Petrenko et al., 2012). The deployment of AERONET-DRAGON sites beginning in 2011 has been a game-changer in terms of the ability to truly consider aerosol spatial variability and the DRAGON deployments at sites around the globe facilitated the analysis presented here.

The performance of the operational V22 17.6 km MISR aerosol retrieval relative to the performance of a prototype 4.4 km retrieval was assessed in comparisons with multiple AERONET-DRAGON deployments over a broad range of AODs. It was found that, overall, the 4.4 km AOD retrieval performed significantly better than the 17.6 km retrieval. In comparisons with AERONET-DRAGON AODs for a variety of globally distributed deployments the 4.4 km resolution retrievals show improved correlation (r = 0.9595), smaller root mean squared error (0.0768), reduced bias (-0.0208), and a larger fraction within the expected error envelope (80.92%). The results for the V22 algorithm are r = 0.8772, RMSE = 0.1683, bias = -0.0887, and 59.09% in the expected error envelope, as shown in Fig. 4. Part of the reason for this improvement is the ability of the higher-resolution retrieval to capture the true spatial variability of the aerosols, which is also captured by the DRAGON networks. Again, a single AERONET site cannot directly represent the spatial variability of aerosols, although this is aliased into the temporal dependence of the AOD observed by the instrument. Averaging the AERONET data over a time window and the satellite data over a spatial window, as is traditionally done in global comparisons, has the effect of minimizing the contributions of true aerosol spatial variability. Another reason for the improvement of the MISR retrieval algorithm when applied at 4.4 km is that the assumptions underlying the aerosol retrieval, particularly over land, are better met at this higher spatial resolution. Ironically, among the most critical of these assumptions is that aerosols are spatially homogeneous on the scale of the retrieval. In other words, aerosol variability itself is likely one of the issues with the 17.6 km retrieval.

The MISR aerosol algorithm team is working toward the release of an updated version of the aerosol retrieval in Spring 2017 that will have results reported globally at 4.4 km resolution. In addition to this change, other changes are being tested and implemented with regard to cloud screening, per-retrieval uncertainty reporting, and microphysical property retrievals. Key to the development of this new algorithm are assessments against a range of cases represented by those used in this paper.

Acknowledgements

This work was performed at the Jet Propulsion Laboratory, California Institute of Technology under a contract with the National Aeronautics and Space Administration. The MISR data used in this work were obtained from the NASA Langley Research Center Atmospheric

Science Data Center. We thank the many PI investigators, and particularly the hard work of Brent Holben and his team for establishing and maintaining the AERONET and AERONET-DRAGON sites used in this investigation. We are also grateful to Dr. Andrew Sayer and an anonymous reviewer for their thoughtful comments that have helped improve this paper.

References

Anderson, T. L., Charlson, R. J., Winker, D. M., Ogren, J. A., and Holmén, K.: Mesoscale variations of tropospheric aerosols, J. Atmos. Sci., 60, 119–136, 2003.

Beyersdorf, A. J., Ziemba, L. D., Chen, G., Corr, C. A., Crawford, J. H., Diskin, G. S., Moore, R. H., Thornhill, K. L., Winstead, E. L., and Anderson, B. E.: The impacts of aerosol loading, composition, and water uptake on aerosol extinction variability in the Baltimore–Washington, D.C. region, Atmos. Chem. Phys., 16, 1003–1015, doi:10.5194/acp-16-1003-2016, 2016.

Bothwell, G. W., Hansen, E. G., Vargo, R. E., and Miller, K. C.: The Multi-angle Imaging SpectroRadiometer science data system, its products, tools, and performance, IEEE Trans. Geosci. Remote Sens., 40, 1467–1476, doi:10.1109/TGRS.2002.801152, 2002.

Boucher, O., Randall, D., Artaxo, P., Bretherton, C., Feingold, G., Forster, P., Kerminen, V.-M., Kondo, Y., Liao, H., Lohmann, U., Rasch, P., Satheesh, S. K., Sherwood, S., Stevens, B., and Zhang, X. Y.: Clouds and aerosols in: Climate Change 2013: The Physical Science Basis. Contribution of Working Group I to the Fifth Assessment Report of the Intergovernmental Panel on Climate Change, Stocker, T. F., Qin, D., Plattner, G.-K., Tignor, M., Allen, S. K., Boschung, J., Nauels, A., Xia, Y., Bex, V., and Midgley, P. M. (eds.), 571–657, Cambridge University Press, Cambridge, United Kingdom and New York, NY, USA, 2013.

Bruegge, C. J., Chrien, N. L., Ando, R. R., Diner, D. J., Abdou, W. A., Helmlinger, M. C., Pilorz, S. H., and Thome, K. J.: Early validation of the Multi-angle Imaging SpectroRadiometer (MISR) radiometric scale, IEEE Trans. Geosci. Remote Sens., 40, 1477–1492, doi:10.1109/TGRS.2002.801583, 2002.

Diner, D. J., Beckert, J. C., Reilly, T. H., Bruegge, C. J., Conel, J. E., Kahn, R. A., Martonchik, J. V., Ackerman, T. P., Davies, R., Gerstl, S. A. W., Gordon, H. R., Muller, J.-P., Myneni, R. B., Sellers, P. J., Pinty, B., and Verstraete, M. M.: Multi-angle Imaging SpectroRadiometer (MISR) instrument description and experiment overview, IEEE Trans. Geosci. Remote Sens., 36, 1072–1087, 1998.

Diner, D. J., Martonchik, J. V., Kahn, R. A., Pinty, B., Gobron, N., Nelson, D. L., and Holben, B. N.: Using angular and spectral shape similarity constraints to improve MISR aerosol and surface retrievals over land, Remote Sens. Environ., 94, 155–171, doi:10.1016/j.rse.2004.09.009, 2005.

Eck, T. F., Holben, B. N., Reid, J. S., Arola, A., Ferrare, R. A., Hostetler, C. A., Crumeyrolle, S. N., Berkoff, T. A., Welton, E. J., Lolli, S., Lyapustin, A., Wang, Y., Schafer, J. S., Giles, D. M., Anderson, B. E., Thornhill, K. L., Minnis, P., Pickering, K. E., Loughner, C. P., Smirnov, A., and Sinyuk, A.: Observations of rapid aerosol optical depth enhancements in the vicinity of polluted cumulus clouds, Atmos. Chem. Phys., 14, 11633–11656, doi:10.5194/acp-14-11633-2014, 2014.

Holben, B. N., Eck, T. F., Slutsker, I., Tanré, D., Buis, J. P., Setzer, A., Vermote, E., Reagan, J. A., Kaufman, Y. J., Nakajima, T., Lavenu, F., Jankowiak, I., and Smirnov, A.: AERONET – A federated instrument network and data archive for aerosol characterization, Remote Sens. Environ., 66, 1–16, 1998.

Ichoku, C., Chu, D., A., Mattoo, S., Kaufman, Y. J., Remer, L. A., Tanré, D., Slutsker, I., and Holben, B. N.: A spatio-temporal approach for global validation and analysis of MODIS aerosol products, Geophys. Res. Lett., 29, 1616, doi:10.1029/2001GL013206, 2002.

Kahn, R. A., Gaitley, B. J., Garay, M. J., Diner, D. J., Eck, T. F., Smirnov, A., and Holben, B. N.: Multiangle Imaging SpectroRadiometer global aerosol product assessment by comparison with the Aerosol Robotic Network, J. Geophys. Res., 115, D23209, doi:10.1029/2010JD014601, 2010.

Kahn, R. A., Nelson, D. L., Garay, M. J., Levy, R. C., Bull, M. A., Diner, D. J., Martonchik, J. V., Paradise, S. R., Hansen, E. G., and Remer, L. A.: MISR aerosol product attributes and statistical comparisons with MODIS, IEEE Trans. Geosci. Remote Sens., 47, 4095–4114, doi:10.1109/TGRS.2009.2023115, 2009.

Kalashnikova, O. V., Garay, M. J., Martonchik, J. V., and Diner, D. J.: MISR Dark Water aerosol retrievals: operational algorithm sensitivity to particle non-sphericity, Atmos. Meas. Tech., 6, 2131–2154, doi:10.5194/amt-6-2131-2013, 2013.

Levy, R. C., Mattoo, S., Munchak, L. A., Remer, L. A., Sayer, A. M., Patadia, F., and Hsu, N. C.: The Collection 6 MODIS aerosol products over land and ocean, Atmos. Meas. Tech., 6, 2989–3034, doi:10.5194/amt-6-2989-2013, 2013.

Limbacher, J. A., and Kahn, R. A.: MISR empirical stray light corrections in high-contrast scenes, Atmos. Meas. Tech., 8, 2927–2943, 2015.

Martin, R. V.: Satellite remote sensing for air quality, Atmos. Environ., 42, 7823 – 7843, doi:10.1016/j.atmosenv.2008.07.018, 2008.

Martonchik, J. V., Kahn, R. A., and Diner, D. J.: Retrieval of aerosol properties over land using MISR observations, in Satellite Aerosol Remote Sensing of Land, Kokhanovsky, A., A., and de Leeuw, G. (eds.), Springer, Berlin, 267–293, doi:10.1007/978-3-540-69397-0_9, 2009.

Munchak, L. A., Levy, R. C., Mattoo, S., Remer, L. A., Holben, B. N., Schafer, J. S., Hostetler, C. A., and Ferrare, R. A.: MODIS 3 km aerosol product: applications over land in an urban/suburban region, Atmos. Meas. Tech., 6, 1747–1759, doi:10.5194/amt-6-1747-2013, 2013.

Petrenko, M., Ichoku, C., and Leptoukh, G.: Multi-sensor Aerosol Products Sampling System (MAPSS), Atmos. Meas. Tech., 5, 913–926, doi:10.5194/amt-5-913-2012, 2012.

Remer, L. A., Mattoo, S., Levy, R. C., and Munchak, L. A.: MODIS 3 km aerosol product: algorithm and global perspective, Atmos. Meas. Tech., 6, 1829–1844, doi:10.5194/amt-6-1829-2013, 2013.

Sano, I., Mukai, S., Nakata, M., and Holben, B. N.: Regional and local variations in atmospheric aerosols using ground-based sun photometry during DRAGON in 2012, Atmos. Chem. Phys. Discuss., doi:10.5194/acp-2016-381, 2016.

Sayer, A. M., Hsu, N. C., Bettenhausen, C., and Jeong, M.-J.: Validation and uncertainty estimates for MODIS Collection 6 “Deep Blue” aerosol data, J. Geophys. Res. Atmos., 118, 7864–7873, doi:10.1002/jgrd.50600, 2013.

Sayer, A. M., Hsu, N. C., Bettenhausen, C., Jeong, M.-J., and Meister, G.: Effect of MODIS Terra radiometric calibration improvements on Collection 6 Deep Blue aerosol products: Validation and Terra/Aqua consistency, J. Geophys. Res. Atmos., 120, 12,157–12,174, doi:10.1002/2015JD023878, 2015.

Seo, S., Kim, J., Lee, H., Jeong, U., Kim, W., Holben, B. N., Kim, S.-W., Song, C. H., Lim, and Lim, J. H.: Estimation of PM_{10} concentrations over Seoul using multiple empirical models with AERONET and MODIS data collected during the DRAGON-Asia campaign, Atmos. Chem. Phys., 15, 319–334, doi:10.5194/acp-15-319-2015, 2015.

Shi, Y., Zhang, J., Reid, J. S., Hyer, E. J., Eck, T. F., Holben, B. N., and Kahn, R. A.: A critical examination of spatial biases between MODIS and MISR aerosol products – application for potential AERONET deployment, Atmos. Meas. Tech., 4, 2823–2836, doi:10.5194/amt-4-2823-2011, 2011.

van Donkelaar, A., Martin, R. V., Brauer, M., and Boys, B. L.: Use of satellite observations for long-term exposure assessment of global concentrations of fine particulate matter, Environ. Health Persp., 123, 135–143, doi:10.1289/ehp.1408646, 2015.

van Donkelaar, A., Martin, R. V., Brauer, M., Hsu, N. C., Kahn, R. A., Levy, R. C., Lyapustin, A., Sayer, A. M., and Winker, D. M.: Global estimates of fine particulate matter using a combined geophysical-statistical method with information from satellites, models, and monitors, Environ. Sci. Technol., 50, 3762–3772, doi:10.1021/acs.est.5b05833, 2016.

Witek, M. L., Garay, M. J., Diner, D. J., and Smirnov, A.: Aerosol optical depths over oceans: A view from MISR retrievals and collocated MAN and AERONET in situ observations, J. Geophys. Res. Atmos., 118, 1–14, doi:10.1002/2013JD020393, 2013.

1 Table 1. Spatial statistics of AERONET-DRAGON deployments.

DRAGON Campaign	Sites	Pairs	Separation < 17.6 km	Separation < 8.8 km	Separation < 4.4 km	Mean Separation (km)	Median Separation (km)
USA 2011 (Washington D.C., Baltimore)	46	1035	105	21	2	51.4	42.6
Asia 2012 (Japan, South Korea)	53	1378	54	22	11	525.9	543.0
SE Asia 2012 (7-SEAS)	46	1035	31	8	3	1927.0	1877.5
USA 2012-2013 (San Joaquin Valley)	28	378	7	3	1	245.7	204.8
Germany 2013 (HOPE)	15	105	3	3	1	359.2	397.4
USA 2013 (Houston)	19	171	6	2	1	103.3	66.1
USA 2013 (SEAC^{4}RS)	54	1431	9	5	3	993.6	989.0
USA 2014 (Colorado)	15	105	6	1	0	87.1	53.1

2

1 Table 2. MISR cases for AERONET-DRAGON comparison.

Orbit	Date/Time	Campaign	SOM Path	MISR Blocks	Notes
60934	2011-06-02 16:05 UTC	Washington, Baltimore	16	58-60	Low AOD, Clear
61633	2011-07-20 16:05 UTC	Washington, Baltimore	16	58-60	Moderate AOD, Scattered Clouds
61662	2011-07-22 15:55 UTC	Washington, Baltimore	14	58-60	Moderate AOD, Scattered Clouds
65440	2012-04-07 02:20 UTC	Asia-Seoul	115	60-62	Low AOD, Clear
65731	2012-04-27 01:55 UTC	Asia-Osaka	111	62-64	Low AOD, Clear
65775	2012-04-30 02:25 UTC	Asia-Seoul	116	60-62	Moderate AOD, Clear
65906	2012-05-09 02:20 UTC	Asia-Seoul	115	60-62	High AOD, Hazy
66139	2012-05-25 02:20 UTC	Asia-Seoul	115	60-62	High AOD, Hazy
69644	2013-01-20 18:50 UTC	San Joaquin Valley	42	60-63	Low AOD, Clear
69877	2013-02-05 18:50 UTC	San Joaquin Valley	42	60-63	Moderate AOD, Few Clouds

2

3

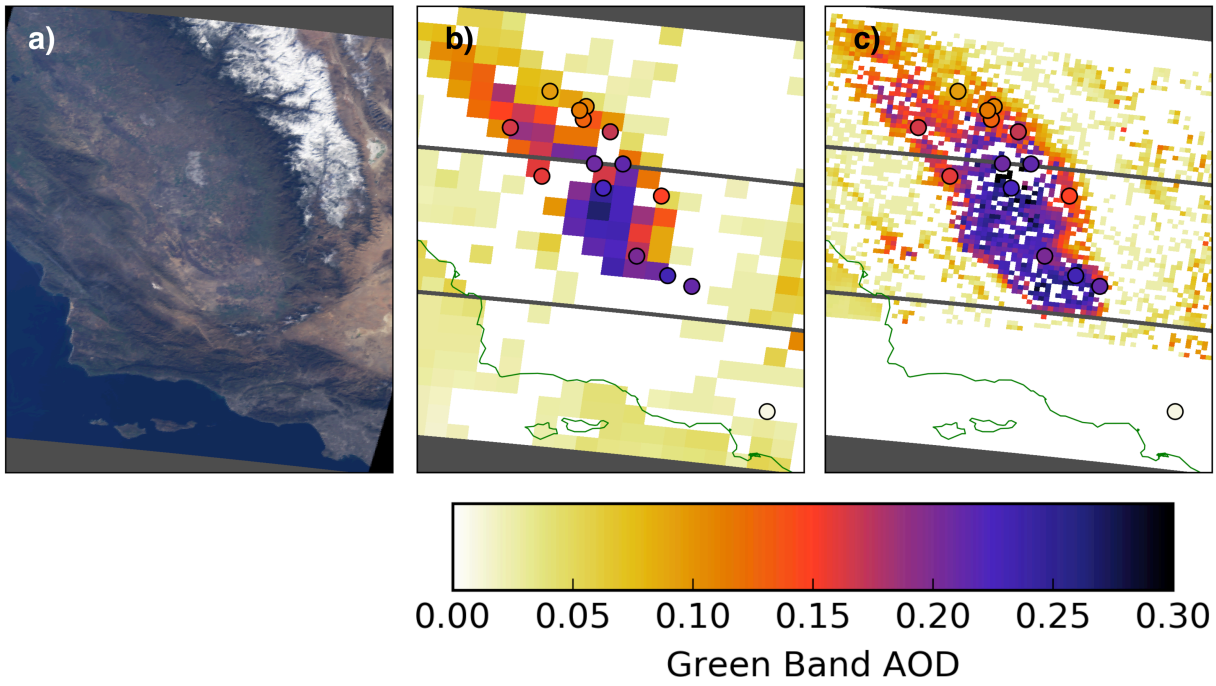

Figure 1. (a) MISR red band image of the San Joaquin Valley in California on 20 January 2013 at around 18:50 UTC; (b) MISR V22 17.6 km aerosol optical depth (AOD); (c) MISR 4.4 km AOD retrieved using the V22 aerosol retrieval algorithm with 275 m local mode data as input.

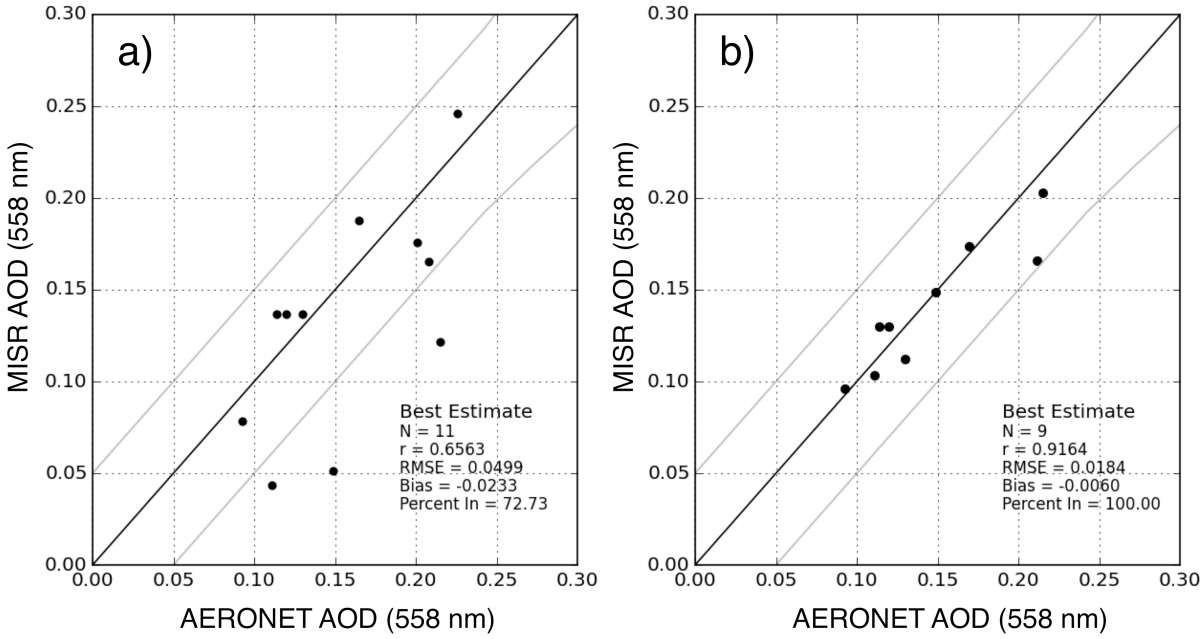

Figure 2. (a) Comparison of MISR V22 17.6 km resolution AODs against AERONET-DRAGON interpolated to the MISR wavelength for 20 January 2013. (b) Comparison of the 4.4 km resolution AODs against AERONET-DRAGON for the same date.

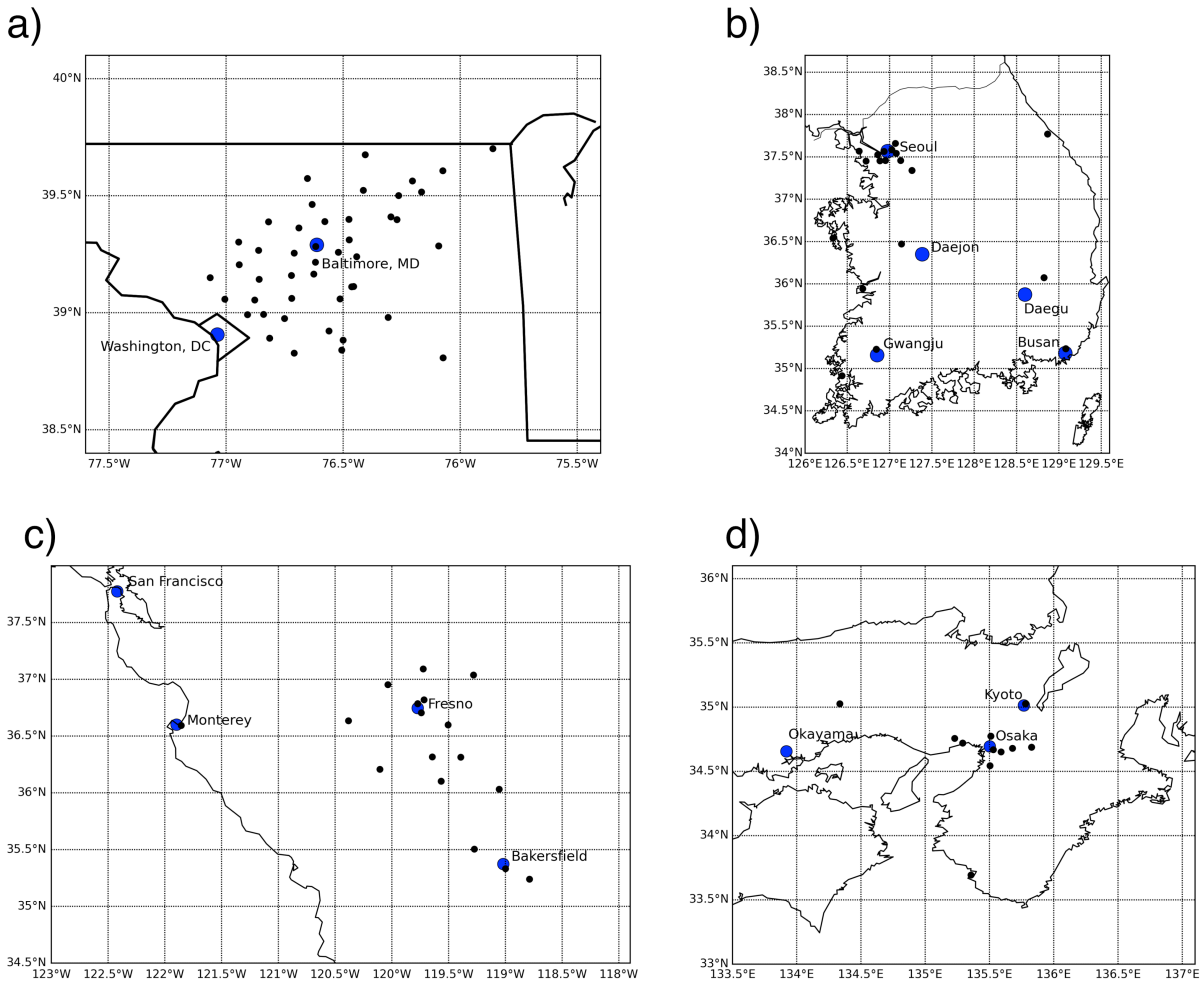

Figure 3. (a) Locations of the 45 sites deployed as part of the AERONET-DRAGON campaign in Washington, D.C./Baltimore metropolitan area; (b) Locations of the 25 sites deployed in South Korea during DRAGON-Asia 2012; (c) Locations of the 18 sites deployed in the San Joaquin Valley in California in late 2012 and early 2013; (d) Location of the 14 sites deployed in Japan during DRAGON-Asia 2012.

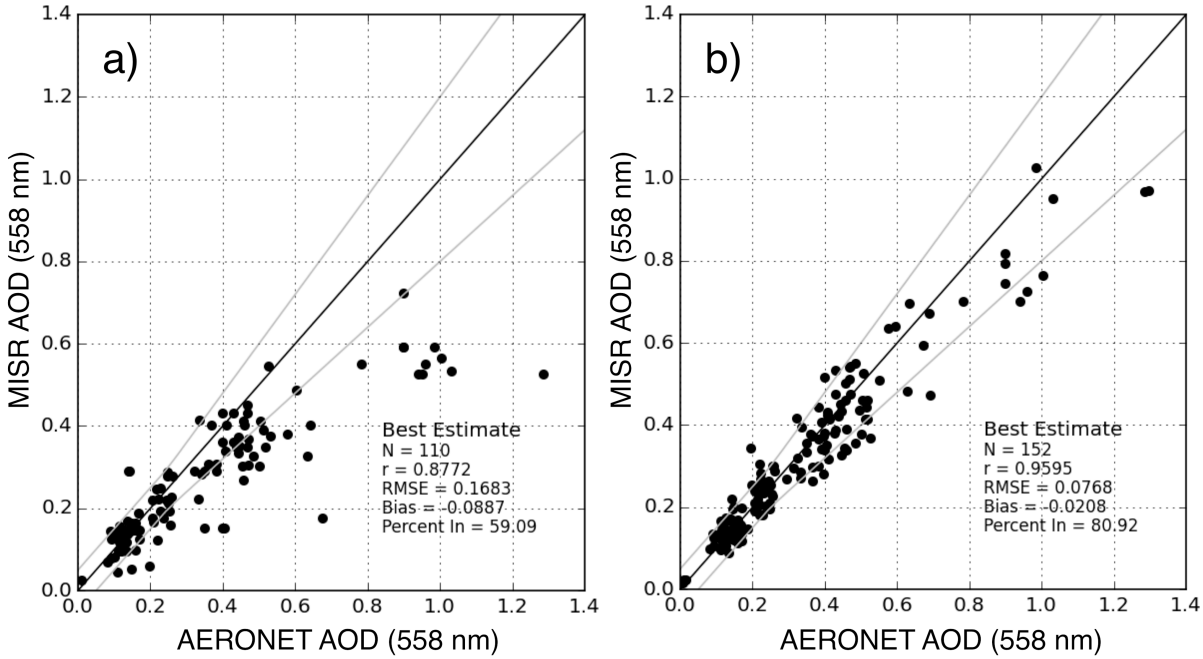

Figure 4. (a) Comparison of MISR V22 17.6 km resolution AODs against AERONET-DRAGON interpolated to the MISR wavelength for all cases shown in Table 2. (b) Comparison of the 4.4 km resolution AODs against AERONET-DRAGON.

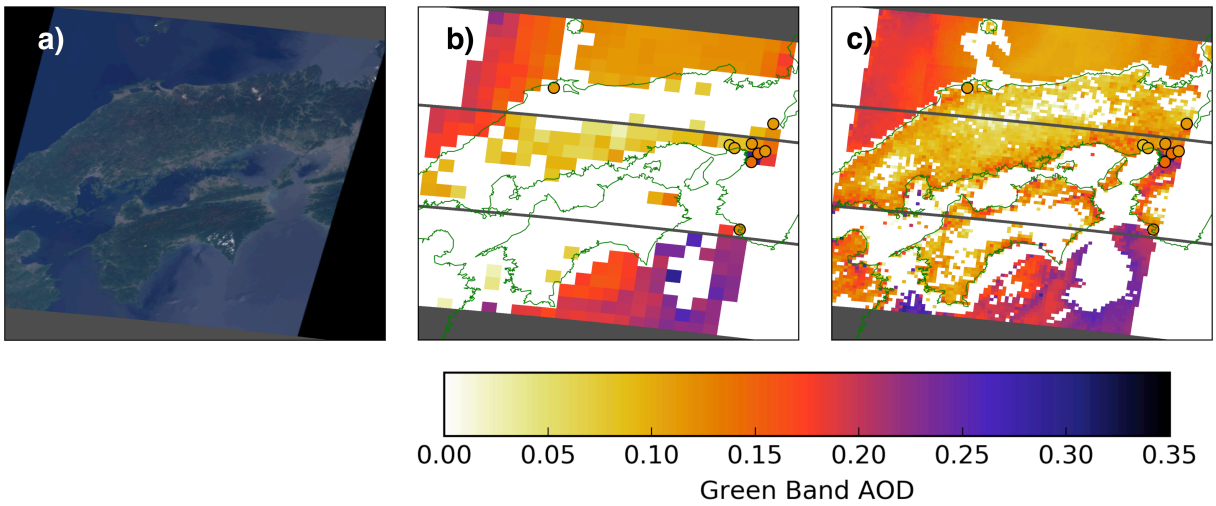

Figure 5. (a) MISR red band image of the Osaka, Japan on 27 April 2012 at around 01:55 UTC; (b) MISR V22 17.6 km aerosol optical depth (AOD); (c) MISR 4.4 km AOD retrieved using a prototype algorithm that takes the 1.1 km resolution global data as input.

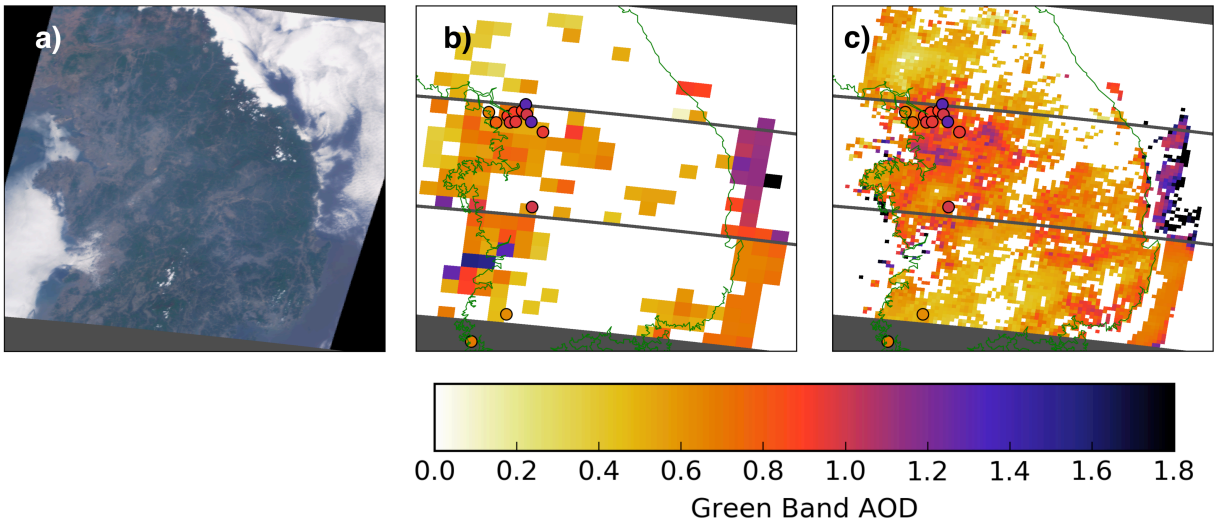

Figure 6. (a) MISR red band image of the Korean peninsula on 09 May 2012 at around 02:20 UTC; (b) MISR V22 17.6 km aerosol optical depth (AOD); (c) MISR 4.4 km AOD retrieved using the prototype algorithm.

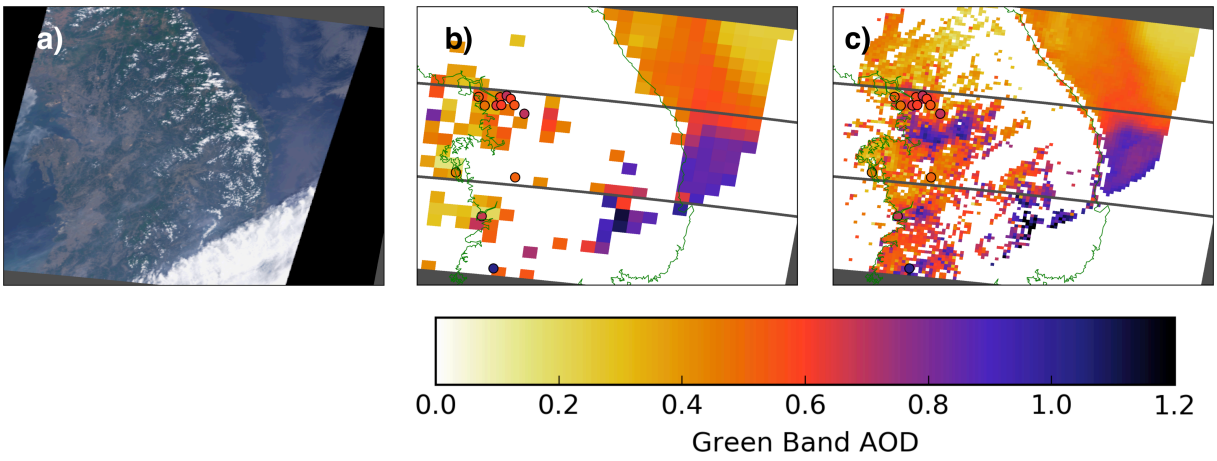

Figure 7. (a) MISR red band image of the Korean peninsula on 25 May 2012 at around 02:20 UTC; (b) MISR V22 17.6 km aerosol optical depth (AOD); (c) MISR 4.4 km AOD retrieved using the prototype algorithm.